



ELSEVIER

Contents lists available at ScienceDirect

## Annals of Nuclear Energy

journal homepage: [www.elsevier.com/locate/anucene](http://www.elsevier.com/locate/anucene)

# Numerical simulation of hydrodynamic performance of taper cascades in transient conditions

Morteza Imani <sup>a,\*</sup>, Mahdi Aghaei <sup>a</sup>, Alireza Keshtkar <sup>b</sup><sup>a</sup> Engineering Department, Shahid Beheshti University, G.C., P.O. Box: 1983963113, Tehran, Iran<sup>b</sup> Nuclear Science and Technology Research Institute, P.O.Box: 11365-8486, Tehran, Iran

## ARTICLE INFO

## Article history:

Received 2 August 2021

Received in revised form 8 May 2022

Accepted 13 June 2022

Available online 20 June 2022

## Keywords:

Finite difference method

Hydrodynamic

Transient condition

Pipe network

Stable isotope separation

## ABSTRACT

The hydrodynamic performance of separation cascades involves determining the distribution of pressure and flow along cascades which are important from the design and operational point of view. In this paper, numerical simulation of hydrodynamic performance of taper cascades in the transient state is presented. This mathematical modeling consisted of a set of hyperbolic partial, ordinary differential and algebraic equations of transient flow in a complex pipe network. In order to achieve this goal, a MATLAB code, named Hydrodynamic Simulation of Separation Cascades (HSSC), has been developed. This code calculates the flow and pressure distribution within the cascade components such as pipes, control valves, tanks and gas centrifuges (GC). Using this code, the results of transient hydrodynamic simulations for a taper cascade with 4 stages and 8 GCs are presented wherein the working gas is xenon, and for different operational conditions, analysis is performed on the equilibrium time and gas holdup.

© 2022 Elsevier Ltd. All rights reserved.

## 1. Introduction

Today, stable isotopes are widely used in industry and medical sciences, and the development of methods for separating them from natural feeds is essential. One of the efficient methods of separating stable isotopes is the use of gas centrifuge cascades (Sulaberidze and Borisevich, 2001). In gas centrifuge cascades, centrifuges are arranged in square and taper structures based on changes in interstage feed flow rate of stages (Manson et al., 1981).

Simulation of separation cascades is the simulation of concentration distribution and hydrodynamic performance of gas within the cascade. In hydrodynamic simulations, the flow and pressure distributions along the cascade are calculated. Hydrodynamic simulation of transient conditions is important in several aspects. In the transient hydrodynamic simulation of the cascade, the cascade equilibrium time and the amount of cascade holdup can be calculated. In the stable isotope separation, it is important to know the equilibrium time and the amount of cascade holdup due to the high price of some isotopes. Using the calculated flows from the hydrodynamic simulation, it is also possible to calculate the concentration distribution within the cascade (Zeng and Ying, 2001). Due to the fact that each GC is designed in its own flow and

pressure range, this tool can be used to identify critical points and GCs that have more pressure than the design value, and it can be used to evaluate the cascade design (Fu et al., 2005). Moreover, it can be used for adjusting the obtained parameters from the optimization of the cascade. There are many publications that are devoted to the optimization of cascade parameters (Ezazi et al., 2020a,b; Imani et al., 2020, 2021a,b; Palkin, 2020). The main output of these works is the determination of flow and concentration distribution along the cascade. However, the optimal parameters need to be adjusted to the cascade by control valves, and the hydrodynamic simulation of cascades in transient and steady conditions can help for this purpose.

In order to perform transient hydrodynamic simulation, the gas flow must be modeled in all components of the cascade. Cascade components include pipes, tanks, control valves, and GCs. In a previous study in 1986, Malik et al. simulated a single GC to study the vibrations of the waste pipe (ALAM et al., 1986). In 1998, Malik et al. provided the mathematical equations which are necessary for transient hydrodynamic simulation (Malik et al., 1998). Using the same method, Zang et al. in 2005 performed a hydraulic simulation of a square cascade (Fu et al., 2005). In 2018, Orlov et al. simulated the distribution of flow and pressure in the cascade, regardless of the pipe network (Orlov et al., 2018). In other cascade-related research, only steady-state conservation of mass balance equations has been used to calculate the flow distribution in the cascade (Azizov et al., 2020; Ezazi et al., 2022; Khoshechin et al., 2021; Mustafin et al., 2020).

\* Corresponding author.

E-mail addresses: [mort.imani@alumni.sbu.ac.ir](mailto:mort.imani@alumni.sbu.ac.ir), [Imani.mrt@gmail.com](mailto:Imani.mrt@gmail.com) (M. Imani).

## Nomenclature

<i>Latin</i>				
<i>A</i>	Cross-sectional area of pipe	<i>f</i>	Darcy friction factor	
<i>B</i>	Dimensional/ units conversion constant	<i>i</i>	Node or mesh number	
<i>P</i>	Pressure	<i>l</i>	Length of pipe	
<i>ṁ</i>	Mass flow rate	<i>V<sub>r</sub></i>	Volume of GC	
<i>C<sub>d</sub></i>	Discharge coefficient	<i>x</i>	Space variable	
<i>C<sub>p</sub></i>	Normal shockwave coefficient at product scope of GC			
<i>C<sub>w</sub></i>	Normal shockwave coefficient at waste scope of GC			
<i>D</i>	Diameter of pipe			
<i>r<sub>1</sub></i>	Internal radius of GC			
<i>r</i>	Ratio of pressure down and upstream of a valve			
<i>R</i>	Gas constant			
<i>t</i>	Time variable			
<i>T</i>	Temperature			
<i>V</i>	Volume of tank			
			<i>Greek characters</i>	
			$\gamma$	Ratio of two specific heats of gas
			$\gamma'$	Ratio of two specific heats of gas
			$\rho$	Density of gas
			$\omega$	Angular velocity of GC
			$\alpha x$	Subscript referring to axis of rotation
			$\alpha v$	Subscript referring to average over entire domain
			$j$	Subscript referring to junction related quantities
			$k$	Subscript referring to pipe number in junction equation

In this paper, numerical simulation of hydrodynamic performance of taper cascades in transient conditions is presented. As a result, a code in MATLAB named HSSC has been developed to perform this simulation. This code calculates the flow and pressure distribution within the cascade components such as pipes, control valves, tanks, and GCs. The secant method is also used to calculate the pressure at the junction of the pipes. The pressure distribution inside GCs is considered exponentially and the finite difference method is used to solve the equations. For control valves, automatic and manual pressure adjustment is also provided. In this work, unlike other researches, pipe networks are considered and pressure regulation at the end of cascades and real boundary conditions for simulation of taper cascades is introduced. By using pressure regulation, different cascade cuts (product to feed flow ratio) are achievable, which leads to having different product concentrations. Finally, using this code, the results of transient hydrodynamic simulation of a taper cascade with 4 stages and 8 GCs are presented wherein the working gas is xenon. For different boundary conditions, analysis is performed on the equilibrium time and gas holdup within the cascade.

## 2. Hydrodynamic simulation of cascade

Fig. 1 shows a schematic of a taper cascade with 8 GCs. The GCs are arranged in four stages, and the feed flow enters from the second stage. As can be seen, there is one control valve on the feed line and two other control valves placed at the outlet of the cascade in the heavy and light flow line. These control valves can control the pressure of a specific location of the cascade.

The feed tank fed the cascade by the operation gas. Light components would be enriched and accommodated in the light tank, and on the other hand, heavy isotopes would be accumulated on the heavy tank. In this figure, the main units are shown and the gas flow inside these components would be simulated.

### 2.1. Gas flow simulation in a pipe

There are 4 governing equations for gas flow in pipes. These are continuity, momentum, energy, and state equation. Considering that the gas flow in the cascade is isothermal, the energy equation can be ignored (Hai et al., 2011; Kiuchi, 1994; Shiono et al., 2019). The continuity and momentum equations for the ideal gas in the one-dimensional system are as follows (Malik et al., 1998).

$$\frac{\partial P}{\partial t} + \frac{RT}{A} \frac{\partial m}{\partial x} = 0 \quad (1)$$

$$\frac{\partial m}{\partial t} + A \frac{\partial P}{\partial x} + \frac{RT}{A} \frac{\partial}{\partial x} \left( \frac{m^2}{P} \right) + \frac{2f_f RT m |m|}{DPA} = 0 \quad (2)$$

Where  $f_f$  is the Fanning friction factor and its relation can be found in (Malik et al., 1998). In Equation (2), the third term is important only in high-velocity ( $Mach \geq 1$ ), and in other cases, it can be omitted. To solve equations (1) and (2), the implicit finite difference method is used. The Crank–Nicolson method is used to discretize the continuity equation, and the fully implicit method is used to discretize the momentum equation, and the following equations are obtained:

$$-\dot{m}_{i-1}^{m+1} + \frac{4A\Delta x}{RT\Delta t} P_i^{m+1} + \dot{m}_{i+1}^{m+1} = \dot{m}_{i-1}^m + \frac{4A\Delta x}{RT\Delta t} P_i^m - \dot{m}_{i+1}^m \quad (3)$$

$$-P_{i-1}^{m+1} + \left( \frac{2\Delta x}{BA\Delta t} + \frac{4RTf_f |\dot{m}_i^{m+1}|}{A^2 BDP_i^{m+1}} \right) \dot{m}_i^{m+1} + P_{i+1}^{m+1} = \frac{2\Delta x}{BA\Delta t} \dot{m}_i^m \quad (4)$$

In the above equations, the superscript  $m$  represents the time interval number, and the subscript  $i$  represents the node number. Moreover, the spatial discretization of equations is based on center difference method. The right side of the above equations is obtained from the previous time step and is known. On the left side, the flow and pressure values in the current time interval are placed that are unknown. The second term in the left side of Equation (4) is nonlinear and to linearize this term, the iteration algorithm is used. This algorithm modifies the coefficient of the nonlinear term in the current time interval. In fact, the nonlinearity arises from the term of  $m^2$  in Eq (2), and by the iteration method, it can be written in the form of  $|m| \times m$  where the  $|m|$  is considered to be known from previous time step and it can be updated by an iteration loop. The superscript \* shows the values from the previous iteration for linearization.

$$-P_{i-1}^{m+1} + \left( \frac{2\Delta x}{BA\Delta t} + \frac{8RTf_f |\dot{m}_i^*|}{A^2 BD(P_{i-1}^* + P_{i+1}^*)} \right) \dot{m}_i^{m+1} + P_{i+1}^{m+1} = \frac{2\Delta x}{BA\Delta t} \dot{m}_i^m \quad (5)$$

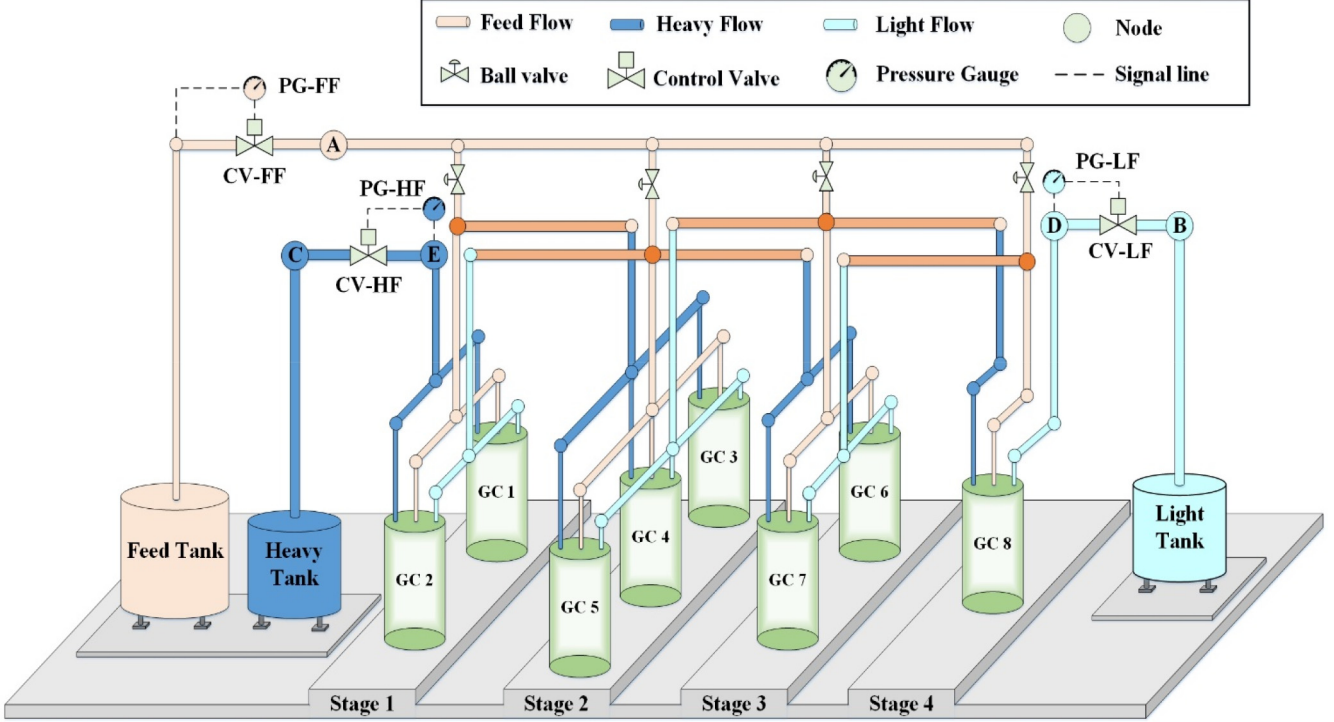


**Fig. 1.** Schematic of a cascade with 4 stages and 8 GCs.

## 2.2. Gas flow simulation in pipes junction

At a pipes junction, the continuity equation must be satisfied. For the control volume considered in Fig. 2, the continuity equation is written as follows:

$$\frac{dP}{dt} + \frac{RT}{V_{node} + \sum_{k=1}^K \Delta x_k A_k} \sum_{k=1}^K \dot{m}_k = 0 \quad (6)$$

In the above Equation  $V$  is the volume of the node at the connection point and  $\sum_{k=1}^K \Delta x_k A_k$  is the volume of the pipes that are in the control volume, and  $K$  is the number of pipes at the connection point.

In steady state, Equation (6) is written as follows.

$$\sum \dot{m}_{out} = \sum \dot{m}_{in} \quad (7)$$

The discretized form of the Equation (6) is obtained as follow:

$$\frac{P_i^{m+1} - P_i^m}{\Delta t} + \frac{RT/2}{V + \sum_{k=1}^K \Delta x_k A_k} (\sum_{k=1}^K \dot{m}_k^{m+1} + \sum_{k=1}^K \dot{m}_k^m) = 0 \quad (8)$$

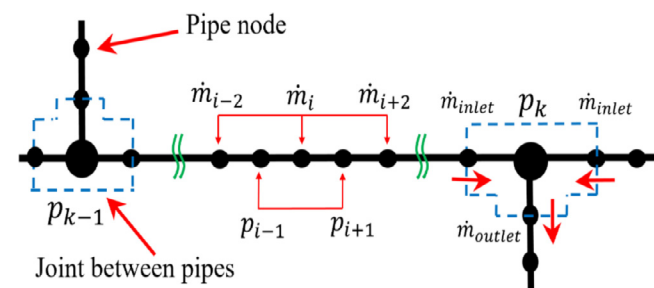


**Fig. 2.** Control volume of the connection point between pipelines.

By arranging the above relation so that the term in  $m + 1$  time interval is placed on the left side, the following equation is obtained:

$$P_i^{m+1} + \frac{\Delta t RT / 2}{V + \sum_{k=1}^K \Delta x_k A_k} \sum_{k=1}^K \dot{m}_k^{m+1} = P_i^m - \frac{\Delta t RT / 2}{V + \sum_{k=1}^K \Delta x_k A_k} \sum_{k=1}^K \dot{m}_k^m \quad (9)$$

by rewriting the above relation:

$$P_i^{m+1} + C_i \sum_{k=1}^K \dot{m}_k^{m+1} = P_i^m - C_i \sum_{k=1}^K \dot{m}_k^m \quad (10)$$

where in the above relation  $C_i$  is as follow:

$$C_i = \frac{\Delta t RT / 2}{V + \sum_{k=1}^K \Delta x_k A_k}. \quad (11)$$

Now according to Equation (10) the error function is defined as follows:

$$E(P_i^{m+1}) = P_i^{m+1} + C_i \sum_{k=1}^K \dot{m}_k^{m+1} - P_i^m + C_i \sum_{k=1}^K \dot{m}_k^m = 0 \quad (12)$$

The pressure that can satisfy the Equation (12) is the pressure at the pipes junction. The  $\sum_{k=1}^K \dot{m}_k^{m+1}$  term is a function of  $P_i^{m+1}$ , so the error function is a nonlinear function of the  $P_i^{m+1}$  term. To solve equation (12), the secant method is used, which is a generalization of the Newton method (Amat et al., 2014; Ji et al., 2020). In this method, two initial guesses of the pressure at the junction of the pipe are needed and the error function is calculated using these pressures. For the next iteration, the pressure can be calculated through the following equation.

$$P_i^{n+1} = P_i^n - E(P_i^n) \frac{P_i^n - P_i^{n-1}}{E(P_i^n) - E(P_i^{n-1})} \quad (13)$$

The secant method is the same as the Newton method, except that the derivative form of the equation is discretized, which therefore requires two initial guesses. The advantage of using the secant method is that there is no need for the derivative of complex equations (Argyros and Khattri, 2013). By using this method, pressure at tanks also can be obtained. In this algorithm, when the error of two consecutive iterations is less than 0.001 the algorithm would stop and the pressure would be the pressure of junction.

### 2.3. Simulation of gas flow in control valves

Simulation of flow when passing through control valves is the same as the simulation of flow when passing through convergent-divergent nozzles. When gas passes through the nozzles, the flow rate through the valve is a function of the pressure before and after the valve and also the cross-sectional area of the valve throat. If the pressure difference before and after the valve is greater than the critical pressure ratio, the flow is subsonic and the flow rate through the valve is calculated according to the following equation (Emmons, 2015).

$$\dot{m} = C_d A_t P_1 \sqrt{\frac{\gamma}{RT} \left( \frac{2}{\gamma - 1} \right) \left( \left( \frac{P_2}{P_1} \right)^{2/\gamma} - \left( \frac{P_2}{P_1} \right)^{(\gamma+1)/\gamma} \right)} \quad (14)$$

If the pressure ratio is less than the critical pressure ratio, the flow would be choked and would not be a function of the pressure after the valve. The maximum flow rate at a constant cross-section of the valve will occur in the chock flow regime. The flow in this case is calculated according to the following equation (Emmons, 2015; Imani et al., 2021b).

$$\dot{m} = C_d A_t P_1 \sqrt{\frac{\gamma}{RT} \left( \frac{2}{\gamma + 1} \right)^{\frac{(\gamma+1)}{(\gamma-1)}}} \quad (15)$$

The critical pressure ratio is defined as the following relation.

$$\frac{P_2}{P_1} = \left( \frac{2}{\gamma + 1} \right)^{\frac{\gamma}{\gamma-1}} \quad (16)$$

### 2.4. Gas centrifuge

For modeling a GC in a cascade, two functions are considered, operation as a tank and operation as a pump. For the tank storage function of GCs, the continuity equation is written as follows (Malik et al., 1998).

$$\frac{dP_{av}}{dt} + \frac{RT}{V_r} (\sum \dot{m}) = 0 \quad (17)$$

Equation (17) assumes an average value for the pressure of a GC because the pressure changes exponentially along the radius of the GC, and it has been shown in the Fig. 3 and the below equation (Nazeer et al., 1999).

$$P_r = P_{av} e^{Zr^2} \quad (18)$$

In the above equation, the value of Z is:

$$Z = \frac{\omega^2}{2RT} \quad (19)$$

In relations (19)  $\omega$  is the rotational speed of the GC and  $r$  is the radial distance from the axis. The average pressure value is calculated as follows:

$$P_{av} = \frac{\int P_r d\nu}{V_r} = \frac{\int P_r d\nu}{\int d\nu} = \frac{P_{av} (e^{Zr_1^2} - 1)}{Zr_1^2} \quad (20)$$

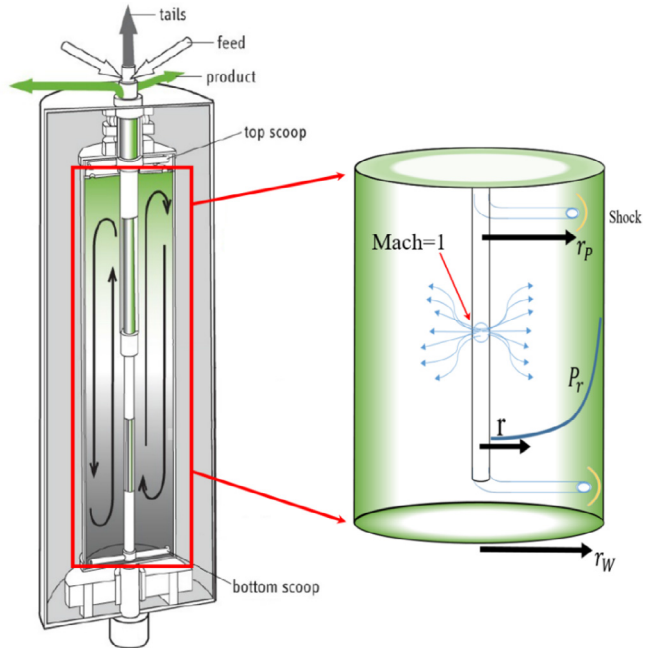


Fig. 3. Schematic representation of a GC and pressure profile inside the GC.

Equation (20) can also be written as follows:

$$P_{av} = P_{av} \frac{Zr_1^2}{(e^{Zr_1^2} - 1)} \quad (21)$$

Therefore, due to the pumping operation of the GC, the pressure in the product and waste scopes is as follows.

$$P_p = P_{av} \frac{Zr_1^2 C_p e^{Zr_p^2}}{e^{Zr_1^2} - 1} \quad (22)$$

$$P_w = P_{av} \frac{Zr_1^2 C_w e^{Zr_w^2}}{e^{Zr_1^2} - 1} \quad (23)$$

In the two above equations, the  $C_p$  and  $C_w$  values are as follows (Emmons, 2015; Fu et al., 2005):

$$C_p = \frac{1}{\gamma + 1} (4Zr_p^2 - (\gamma - 1)) \quad (24)$$

$$C_w = \frac{1}{\gamma + 1} (4Zr_w^2 - (\gamma - 1)) \quad (25)$$

Where  $r_w$  is the radial distance of the waste scope and  $r_p$  is the radial distance of the product scope. The  $C_p$  and  $C_w$  coefficients are applied to take into account the normal shock effect created at the moment the gas enters the waste and product scope. After presenting how to calculate the pressures at the inlet of the scope pipes, another important point regarding the simulation of the GC is how the feed enters the GC. Due to the fact that in the GC, the central pressure of the GC is very low, gas enters the GC in the choked flow condition, and the Mach number at the end of the feed pipes will be 1. Therefore, the Mach number boundary condition is used to simulate the flow in this pipe. The Mach number condition at the end of the pipe is applied as follows (ALAM et al., 1986).

$$Mach = \frac{v}{v_{sound}} = \frac{\frac{\dot{m}}{\rho A}}{\sqrt{\gamma RT}} = 1 \quad (26)$$

By placing the ideal gas relationship instead of density in the above relationship, a relationship between flow and pressure at the end point of the pipe can be obtained as Eq (27), and the resulting relationship can be used as a boundary condition in solving the flow of inlet feed pipe to the GC.

$$P = \frac{RT}{A\sqrt{\gamma RT}} \dot{m} \quad (27)$$

## 2.5. Simulation algorithm

The transient hydrodynamic simulation algorithm is shown in Fig. 4. In this code, first, the input parameters are read, and then the initial conditions of the components are applied. In the next step, boundary conditions are applied to all pipes. If pipes are located at the output flow of GCs, the pressures are determined according to the equations in Section 2.4. In the next step, the pressure of junctions and tanks (including the average pressure of the GCs) is guessed, and with these pressures, the linear equations for all the pipes are solved. According to the calculated flow rates and pressures, the system of linear equations is modified and the process should continue until the convergence of the results. With the convergence of flow and pressure, the solution process is completed for a time step. The values of the boundary and initial conditions are updated for the next time step until the steady-state is reached.

## 3. Validation

In order to validate the HSSC code, one approach can be using MATLAB Simulink to model a simple test and then comparing the results between the MATLAB Simulink and HSSC code. MATLAB Simulink has a section named Simscape for simulation of physical models. Although Simscape has a powerful database and pre-defined components for modeling physical models, it cannot be used for complex pipe networks like cascades. It is only possible by considering many assumptions and simplification. However, it can be employed for a simple network like a single GC connected to tanks. In the gas section of Simscape, there are available components that can be used to model a GC connected to the feed, light, and heavy tank. To create this model, four types of components are used: pipe, constant volume chamber, compressor, and orifice that can be used as a control valve. It has been assumed that the feed, light, and heavy tank have constant pressure and the appropriate component for modeling in Simulink is a reservoir component. For GC modeling, a combination of a constant volume chamber and two compressors connected to this chamber can model a GC. The pressure of these two compressors can be varied based on the average pressure of the chamber and coefficient that can be derived from Eq (22) and Eq (23). So, in Fig. 5, a GC that is connected to associated tanks is shown.

Moreover, in the model, three mass flow sensors and pressure gauges are placed in order to display the results. On the other hand,

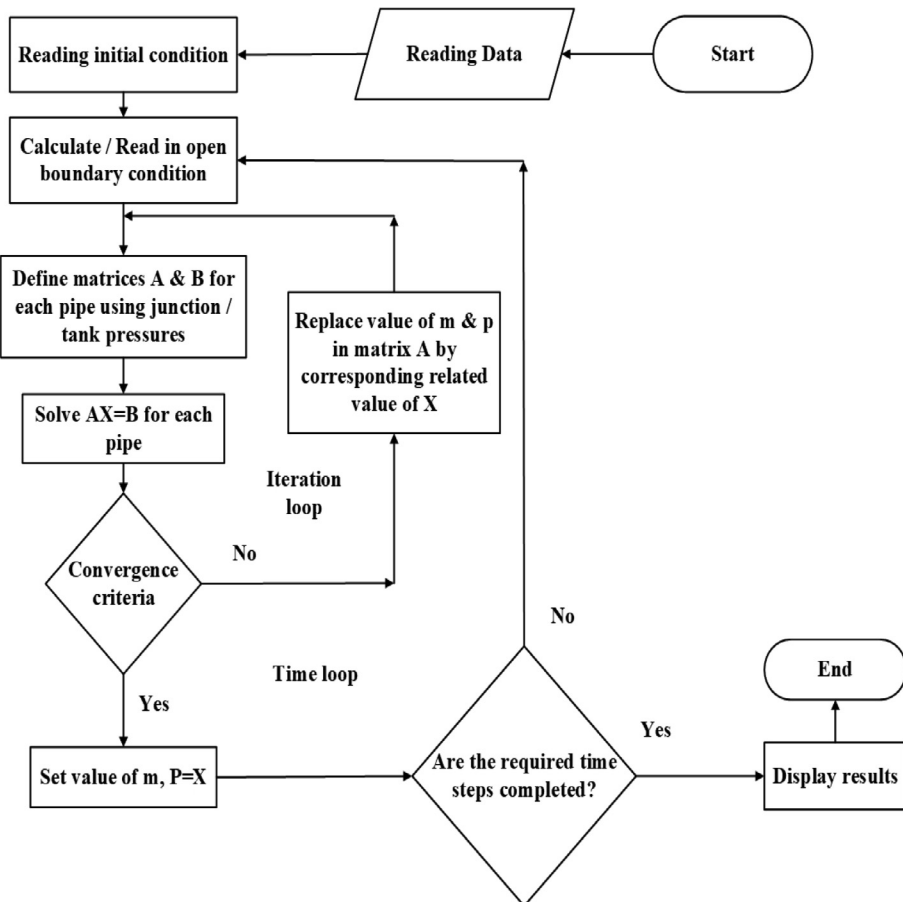


Fig. 4. The algorithm of the HSSC Code.

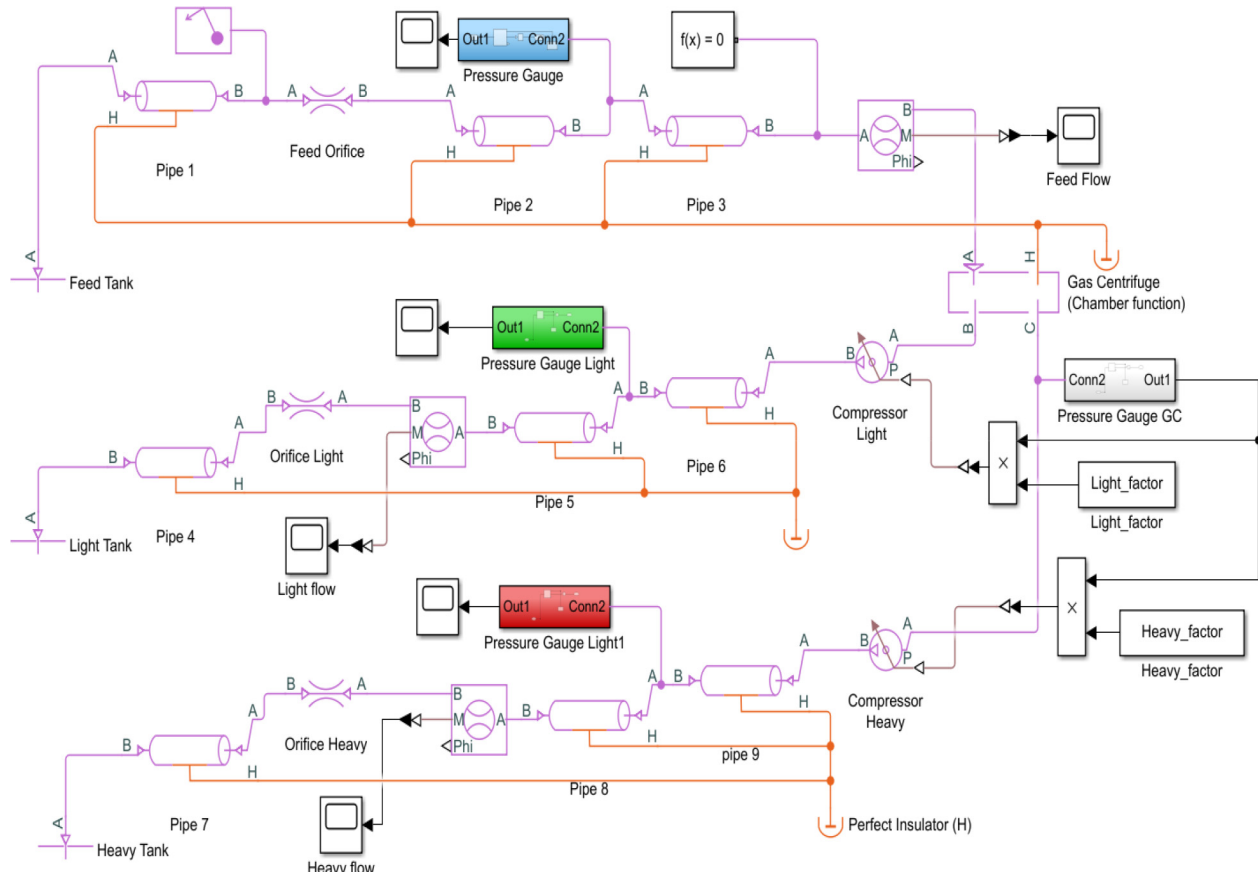


Fig. 5. Simscape model of a single GC connected to feed, light, and heavy tanks.

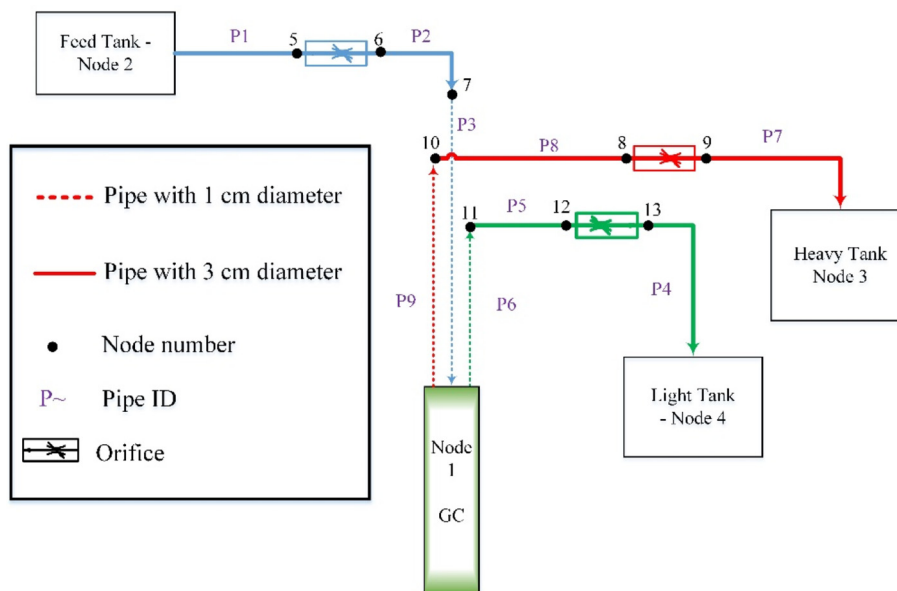


Fig. 6. The model created in the HSSC code for verification.

this model has been created in the HSSC code by the configuration shown in Fig. 6. There are three boundary conditions in this model; the pressure of feed, light, and heavy tanks. These are 400, 1, 1 Pa respectively. The length of each pipe is equal to 1 m and the diameter of the pipes that are directly connected to the GC is 0.01 m, and all the other pipes are 0.05 m. The cross-section of all the orifices is

considered to be equal to  $1e-5 \text{ m}^2$ . The pressure of the feed reservoir also changed to 600 Pa in a second test. In Fig. 7a, the results of the two models have been shown for 50 s. Fig. 7b represents the relative error of the two methods. Furthermore, the simulation has been done for these two methods by considering a change in the pressure of the feed tank from 400 Pa to 600 Pa. The results of these

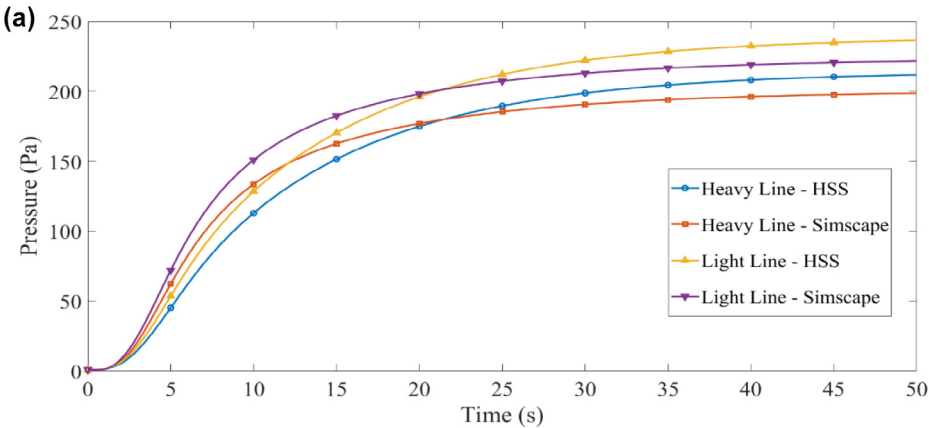


Fig. 7a. The pressure of light (node 11) and heavy (node 10) lines for HSSC code and Simscape (for 400 Pa pressure at the input port).

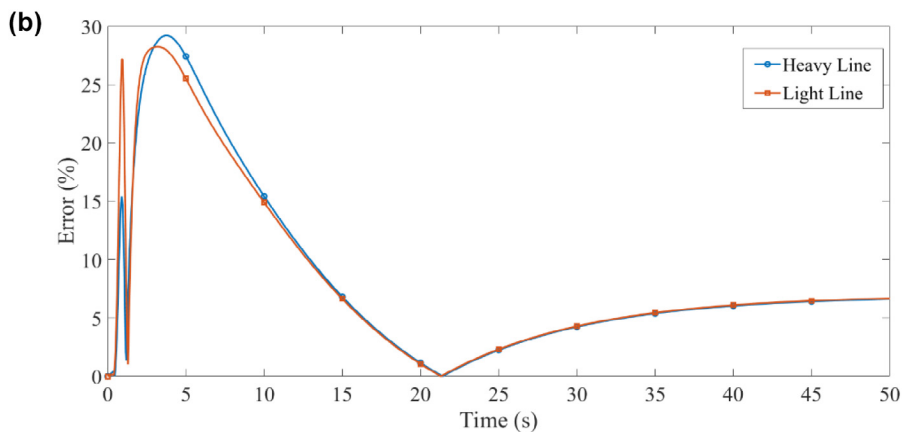


Fig. 7b. The relative error between HSSC code and Simscape results (for 400 Pa pressure at the input port).

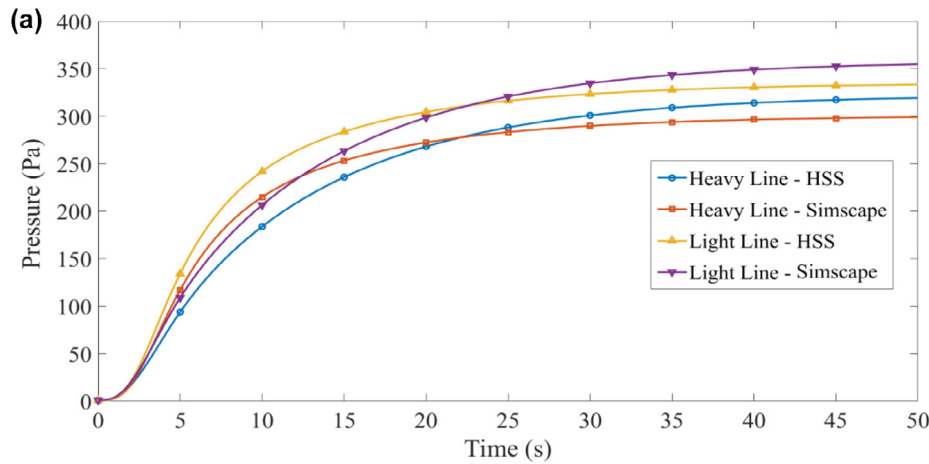


Fig. 8a. The pressure of light (node 11) and heavy (node 10) lines for HSSC code and Simscape (for 400 Pa pressure at the input port).

simulations are presented in Fig. 8. As can be seen from Figs. 7 and 8, the average error over time is less than 10 %, and the steady-state results also have less than 7% relative error. These differences arise from using different friction factor calculations and the fact that the MATLAB Simulink considers an average value of friction for the whole pipe; however, in the HSSC code, the pressure and flow are solved over the length of pipe. In conclusion, based on these results, the two methods are consistent with each other.[Figs. 8a and 8b](#)

#### 4. Results

In this section, the results of simulating a taper cascade with 8 GCs and 4 stages are presented. The working gas is Xenon and its properties can be found in ([Mountain, 2007](#)). The schematic of the cascade used is as shown in [Fig. 1](#). In this section, to simulate this cascade in HSSC code, all pipes and nodes are numbered according to [Fig. 9](#).

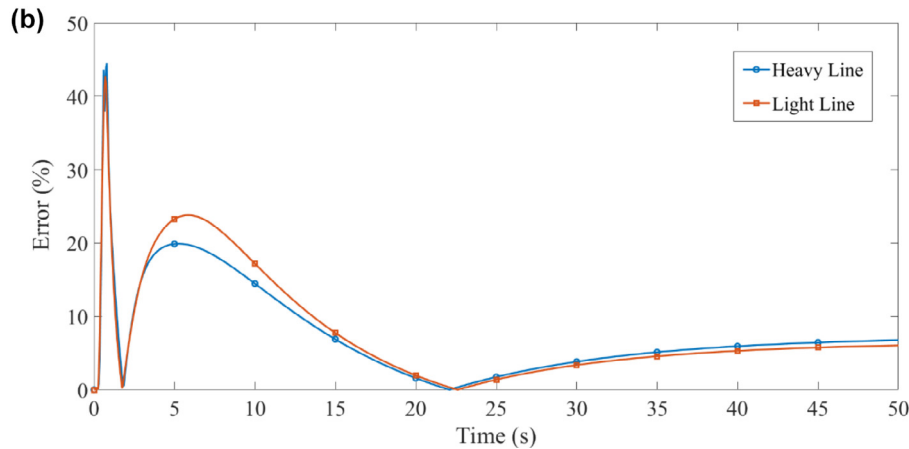


Fig. 8b. The relative error between HSSC code and Simscape results (for 400 Pa pressure at the input port).

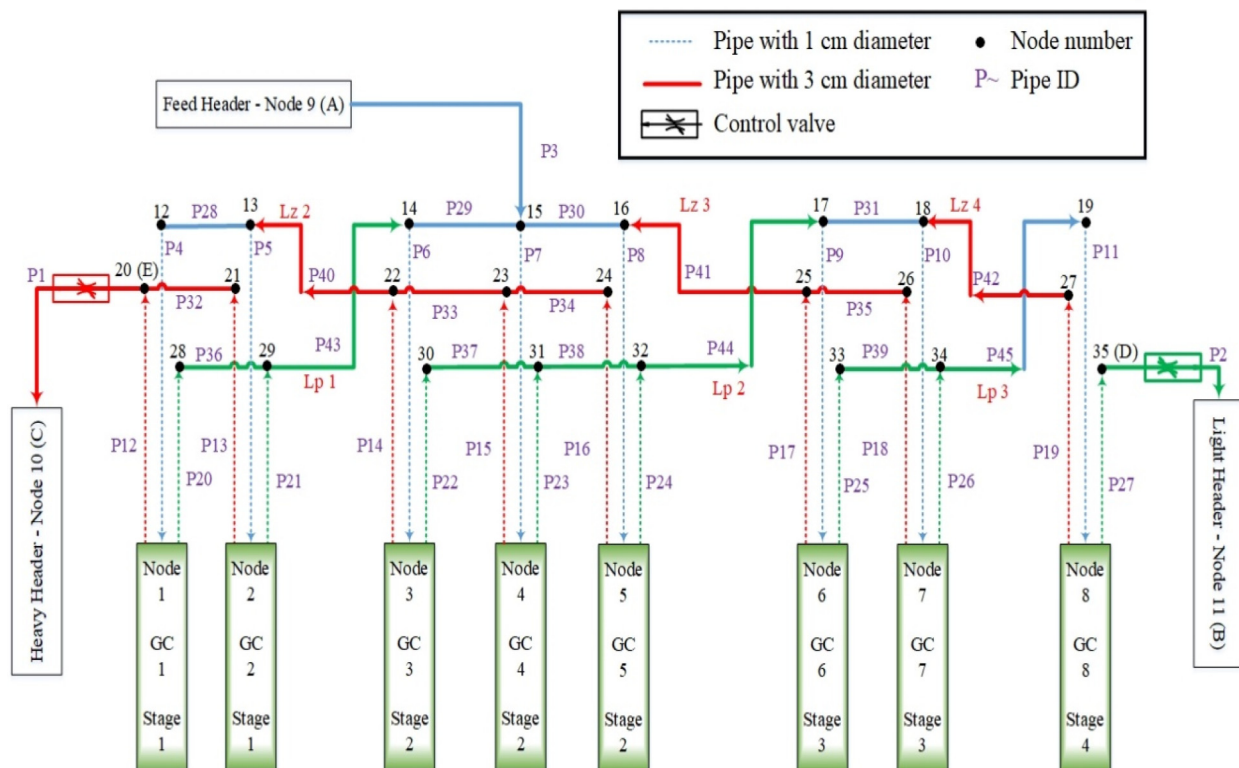


Fig. 9. The numbering of nodes and pipes for the cascade.

According to Fig. 9, 35 nodes, 45 pipes, and 8 GCs have been used in this cascade. The arrangement of GCs in the cascade is 2: 3: 2: 1, and the feed location is the second stage. Two control

valves are placed on the output flow of the cascade (the Heavy and light sides of the cascade). The amount of pressure after the control valves (at nodes B and C) in all tests provided is considered constant at 1 Pa. The reason for this choice is the presence of Roots pumps in this part of the cascade that pumps the output flows to collect in the tanks. The suction pressure of these pumps is considered to be 1 Pa. So, there are three boundary conditions: one mass flow at node A and two output pressure at nodes B and C, in which the pressure boundaries are constant and the mass flow rate varies for each test case. The length of all available pipes is considered 1 m. Table 1 shows the specifications of the GCs. The number of meshes used for all pipes is the same and equal to 30. The initial conditions of the flow rates of all pipes are considered zero and the initial pressure is equal to 1 Pa.

Table 1  
The GC specifications.

Value	Parameter
60 mm	radius
54 mm	$r_p$
56 mm	$r_w$
600 m/s	Velocity
480 mm	Height

#### 4.1. Test case 1

In this test, the amount of input flow to the cascade is considered equal to 75 g/h. By performing the simulation, the cascade reaches equilibrium after 74 s. Fig. 10 shows the average pressure of the GCs over time. According to this figure, GC No. 8 had a lower pressure than the others, and its pressure increases later than the others. The reason is that this GC is far from the feed location. Fig. 11 shows the inlet flow to the GCs in terms of time. As can be seen, the flow rate of GCs in stage 2 has increased rapidly compared to other stages, and the highest input feed flow enters this stage. The critical stage is typically defined as a stage that the GCs of this stage have the maximum feed flow rate and the possibility of a crash is higher than other stages accordingly. So, in the proposed cascade, the second stage is the critical stage.

In this test, the amount of input flow to the cascade is considered to be fixed equal to 75 g / h. By performing the cascade simulation, it reaches equilibrium after 74 s. Fig. 10 shows the average pressure of centrifuges over time. According to this figure, centrifuge No. 8 had a lower pressure than the others and increased the pressure later than the others. The reason for this is that this machine is far from the feed entry stage. Fig. 11 shows the inlet flow to centrifuges in terms of time. As can be seen, the flow rate of stage 2 machines has increased rapidly compared to other stages, and the highest input feed flow enters this stage.

Fig. 12 shows the holdup of the GCs in terms of time. This figure follows Fig. 10 because these two parameters are related to each other. The GCs of stage 2 that have the highest flow and pressure as shown in Fig. 12 also have the highest amount of gas holdup. Fig. 13 shows the total holdup of GCs and pipes over time. According to Fig. 13, the amount of steady-state holdup of gas in the cascade is 0.25 gr.

Fig. 14 shows the pressure before the control valves. As can be seen, the pressure of the heavy flow output is higher than the light flow output due to its proximity to the feed location and the greater number of GCs. In addition, the heavy line pressure starts to increase after about one second, while for the light flow output this happens after 3 s.

Fig. 15 shows the input and output flow of the cascade along with interstage flows. According to this figure, in the first moments (the first 7 s) due to the empty centrifuge machines, the pressure at the output of the first and third stage GCs is low, and therefore the flow enters the GC of these stages in addition to the feed pipe from the product and waste scope. Over time, as the gas holdup in these GCs increases, the pressure at the outlet of them increases, and the

flow direction is corrected. Functionally, the entry of flow from the product and waste scope will increase the vibrations of the centrifuge and will not be desirable (Zhao and Zeng, 2006). Also, it can be seen, the light output flow is 27 g/h and the heavy output flow is 48 g/h. Therefore, the cascade cut (the product flow to feed flow ratio of the cascade) is  $(\frac{27}{75})0.36$ . Fig. 16.

#### 4.2. Test case 2

In this test, the input feed flow has been considered to change according to the following relationship with time.

$$\begin{aligned} \dot{m} &= 3(\text{g}/\text{h}) & t < 5 \\ \dot{m} &= 4.8t - 21(\text{g}/\text{h}) & 5 \leq t < 20 \\ \dot{m} &= 75(\text{g}/\text{h}) & 20 \leq t < 120 \\ \dot{m} &= -2.4t + 363(\text{g}/\text{h}) & 120 \leq t \leq 150 \\ \dot{m} &= 3(\text{g}/\text{h}) & t > 150 \end{aligned} \quad (24)$$

Fig. 12 shows the interstage flows and the input and output flow of the cascade. Comparing Figs. 11 and 12, it can be seen that in test 2, the undesirable input flow from the scopes is reduced. Because the amount of feed is low in the first seconds and gradually increases, the pressure of the GCs in the feed location gradually increases and prevents the inverse flow. According to this figure, the amount of inverse flow is reduced to one-third. Once the amount of input feed is constant, the flows inside the cascade reach a steady state at 100 s, then from 120 to 150 s the cascade feed flow decreases linearly. In this example, the feed flow function shows the commissioning and decommissioning gas supply to the cascade. According to the figure, in the decommissioning phase, the flows of the adjacent stage to the feed location (stages 1 and 3) increase slightly and then begin to decrease. This is the opposite of the commissioning phase.

Fig. 17 shows the pressure before the control valves. According to this figure, in the steady-state condition, the cascade has a pressure more than the initial state where the pressure of the whole cascade was considered to be 1 Pa. Fig. 18 shows the inlet flow to the GCs and Fig. 19 shows the total gas holdup of the cascade.

#### 4.3. Test case 3

In this test, unlike previous tests, an automatic function is considered for control valves and the cross-sectional area of the valve

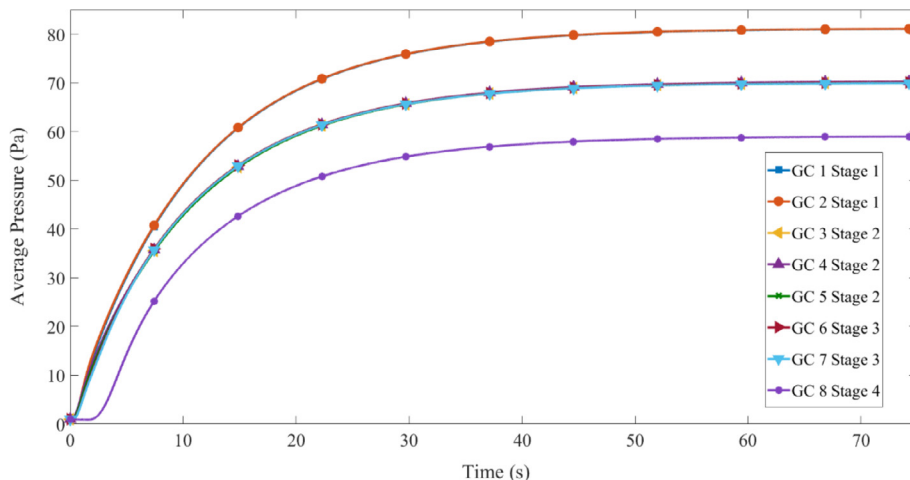


Fig. 10. Average pressure of GCs over time for test case 1.

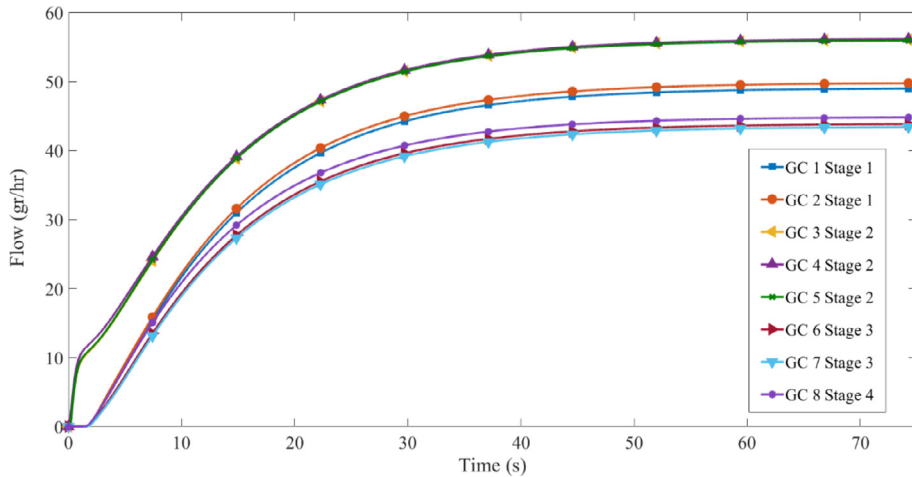


Fig. 11. Inlet flow to GCs from input feed node for test case 1.

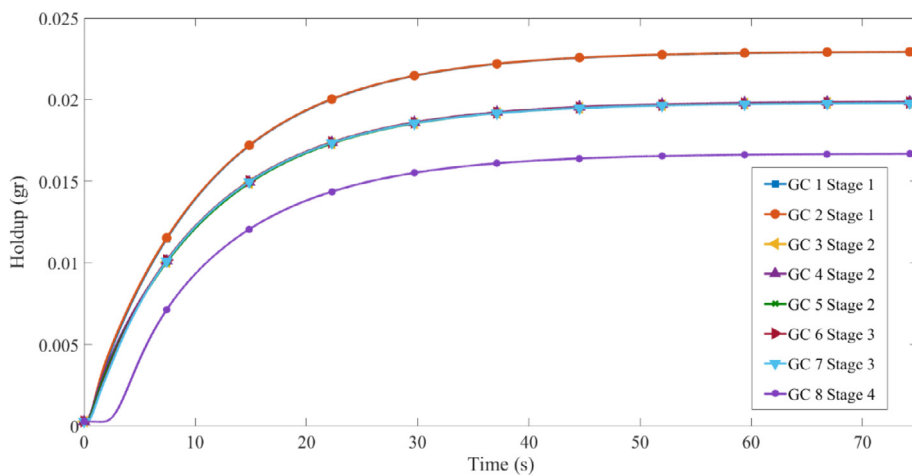


Fig. 12. Holdup of GCs for test case 1.

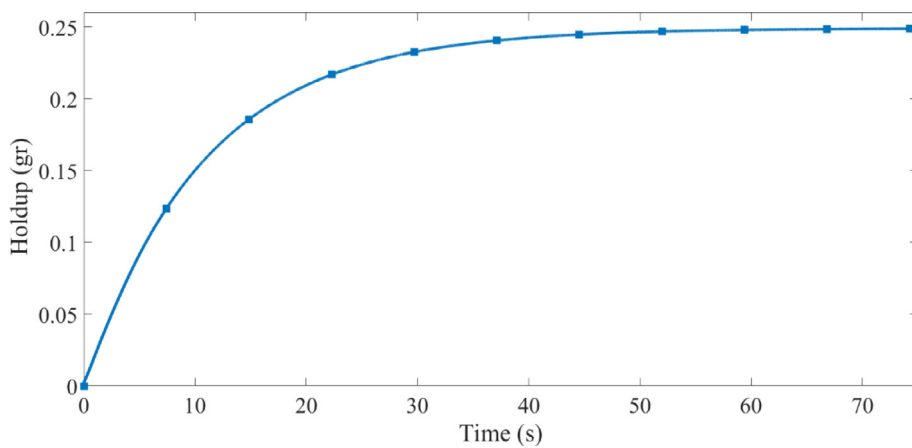


Fig. 13. Total gas holdup of the cascade in terms of time for test case 1.

varies. The control valves are initially completely closed. The light output flow has a pressure setting of 200 Pa at node D and the heavy output flow has a pressure setting of 250 Pa at node E. Fig. 20 shows the algorithm for how the valve adjust the pressure. The response time for the valves is considered 0.1 s and the cross-sectional change is  $2e-7 \text{ mm}^2$  for each response.

Fig. 21 shows the cross-sectional area calculated in time for the two control valves. Fig. 22 also shows the amount of pressure at nodes D and E where the pressure at these points must be adjusted by the control valves. According to these two figures, the pressure of the heavy line reaches 250 Pa in 7.5 s, and the control valve of this line begins to open the valve to reduce the pressure according

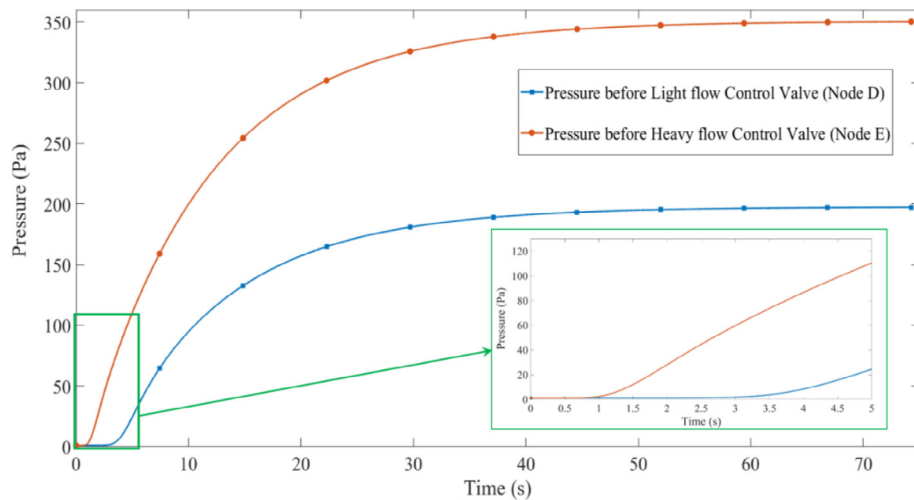


Fig. 14. Pressure of the outlet flows before the control valves in terms of time for test case 1.

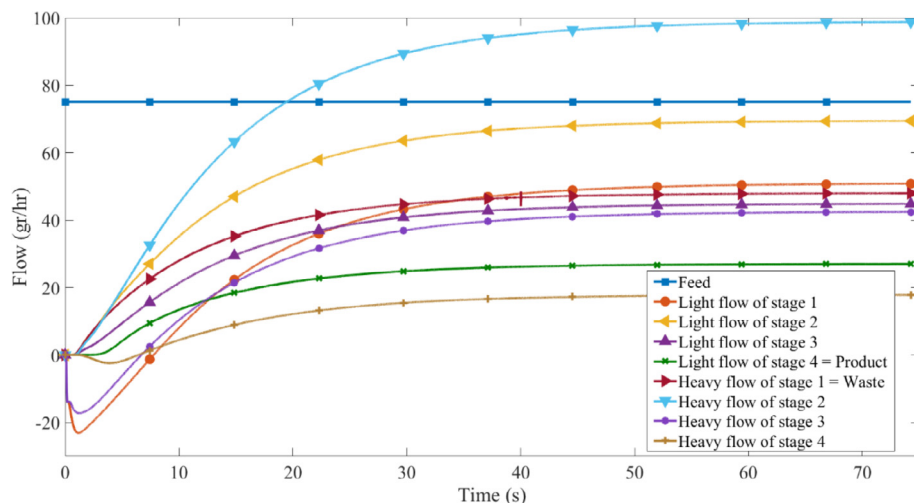


Fig. 15. The input and output flows of the cascade along with the interstage flows for test case 1.

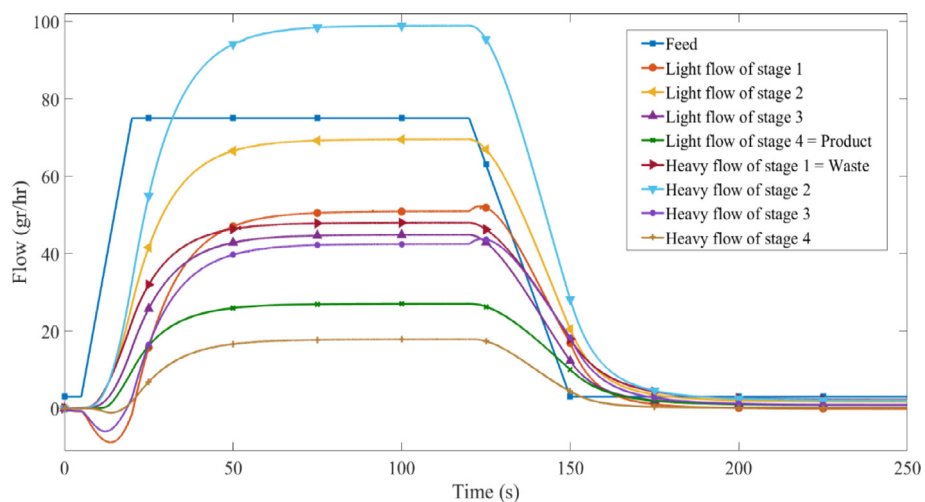
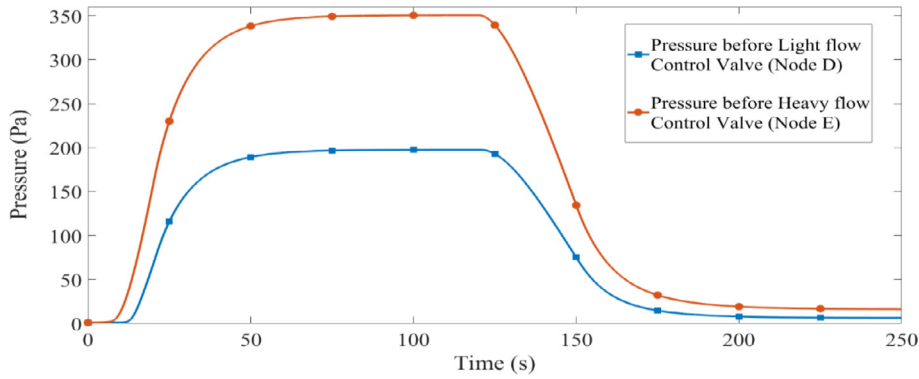
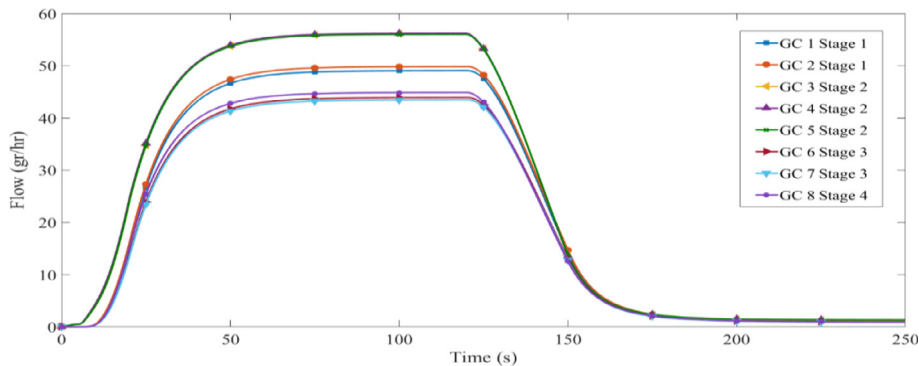


Fig. 16. Input and output flows of the cascade along with interstage flows for test case 2.



**Fig. 17.** Pressure of the outlet flows before the control valves in terms of time for test case 2.



**Fig. 18.** Inlet flow to GCs from the input feed node for test case 2.

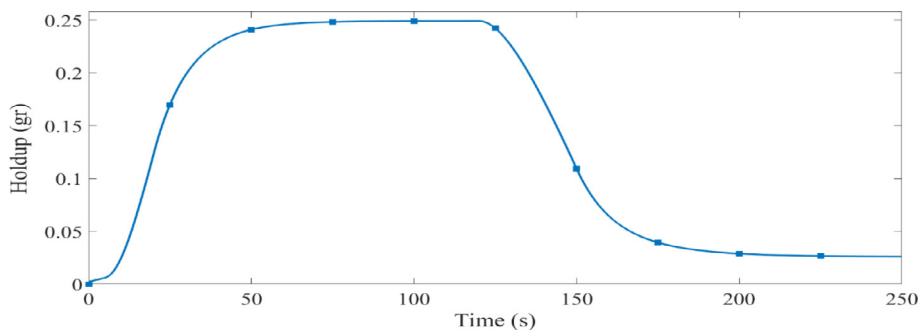


**Fig. 19.** Total gas holdup of the cascade in terms of time for test case 2.

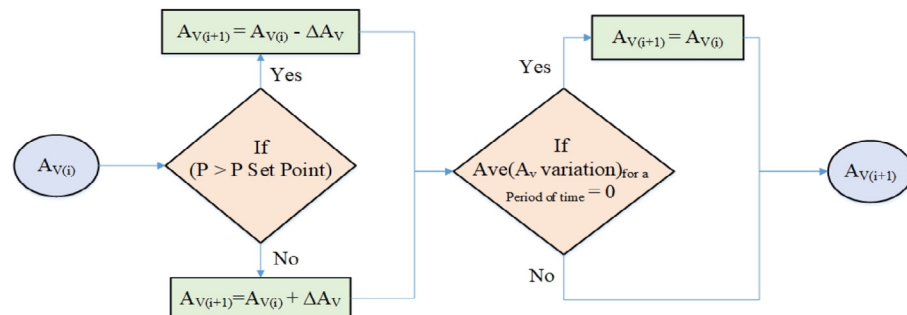


**Fig. 20.** The algorithm for the determination of the cross-sectional area of the control valve.

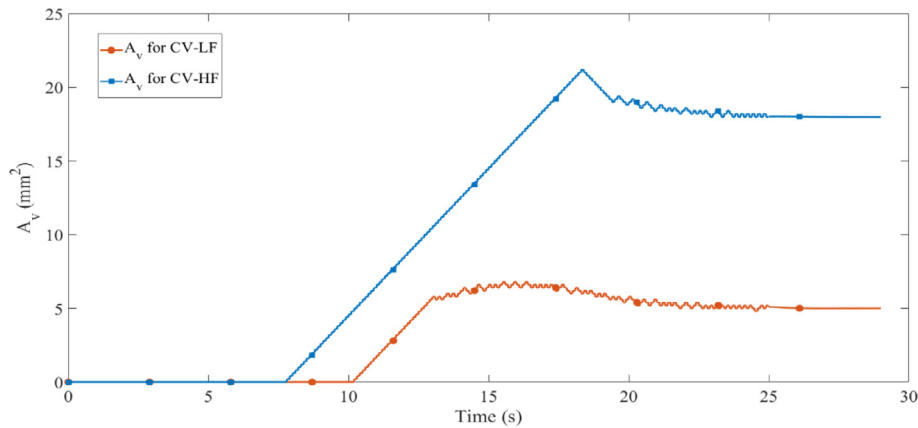


**Fig. 21.** The cross-sectional area of the control valves in terms of time.

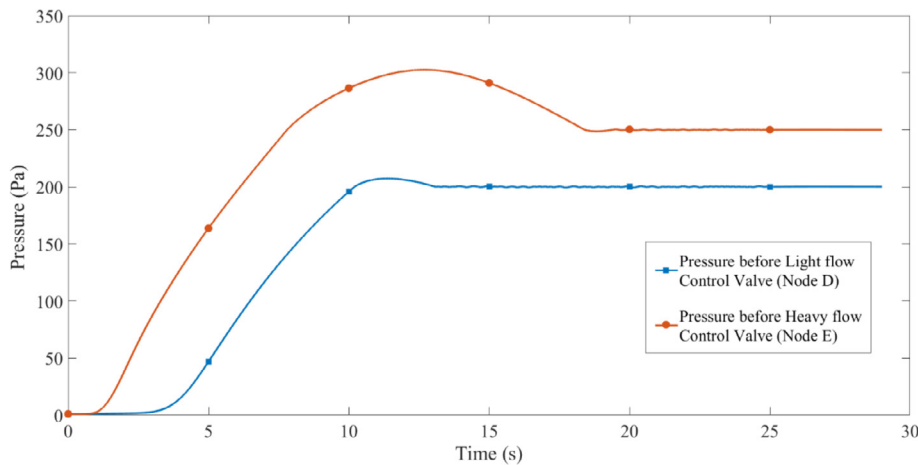


**Fig. 22.** Pressure of the outlet flows before the control valves in terms of time for test case 3.

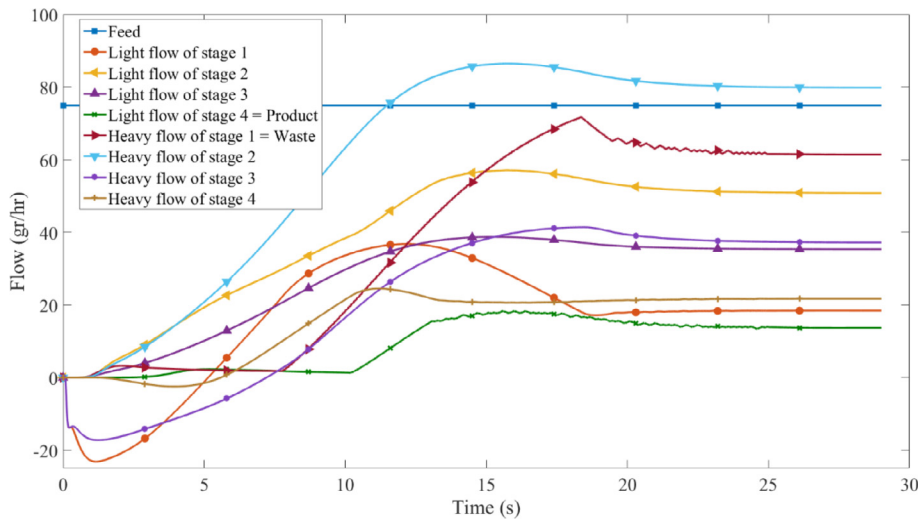


**Fig. 23.** Input and output flows of the cascade along with interstage flows for test case 3.

to the algorithm of Fig. 20. Due to the fact that the rate of increase of pressure is higher than the rate of valve response, the pressure of this line increases to 300 Pa. From 18 s, the pressure drop is greater than the set value and the cross-sectional area of the valve decreases. After repeating this process several times, the pressure

value of this line is fixed after 25 s and the cross-sectional area of this valve remains constant at 18 \$\text{mm}^2\$. This process is also used for the light output line. The difference is that this valve opens in 10 s, and in steady-state, the opening value of the valve is 5 \$\text{mm}^2\$. According to Fig. 23, the light output flow is 13 \$\text{g}/\text{h}\$ and

the heavy output flow is 62 g/h in steady-state condition. In this test, adjusting the pressure of the control valves has led to a cascade cut equals to 0.173 ( $\frac{13}{75} = 0.173$ ). Therefore, by adjusting the pressure of the control valves, different and desired cascade cut can be applied to the cascade. By comparing tests 1 and 3, it can be seen that adjusting the pressure in the specified value causes the cascade cut to decrease from 0.36 to 0.173. Also, equilibrium time and total gas holdup of the cascade are reduced as well.

**Fig. 23** shows the Input and output flow of the cascade along with interstage flows for this test. According to this figure, the out-

put flows of the cascade fluctuate. These fluctuations are due to the variation of control valves' cross-sectional area. The frequency of these oscillations is the same as the frequency of the cross-sectional area changes of the control valves. These fluctuations are damped due to the tank storage operation of the GCs and are not seen in other places.

**Fig. 24** shows the holdup of each GC in terms of time. By comparing Figs. 20 and 8, it can be seen that in test 3 the amount of gas holdup reduced, and it can be concluded that the pressure distribution in the cascade is lower than in test 1.

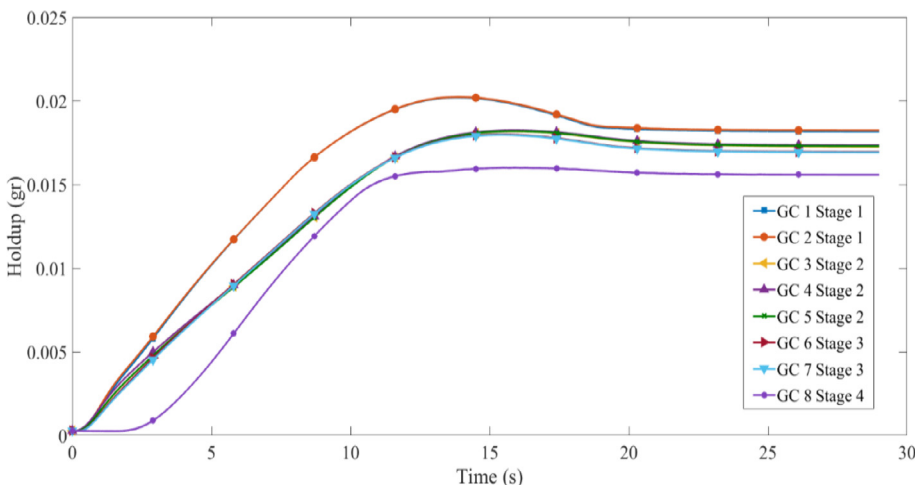
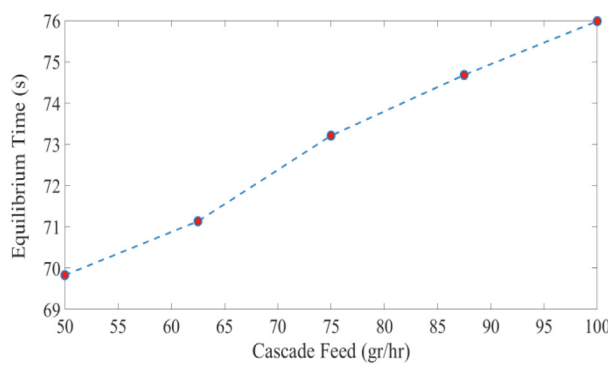
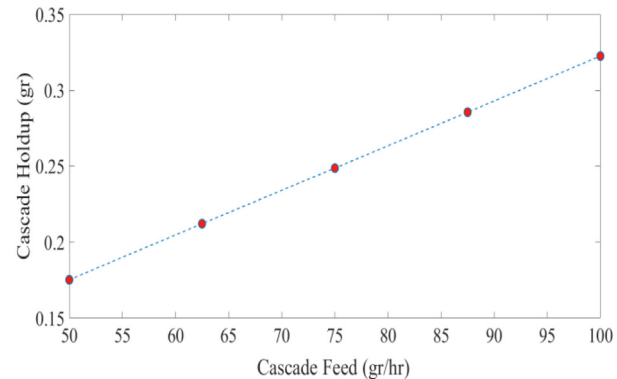


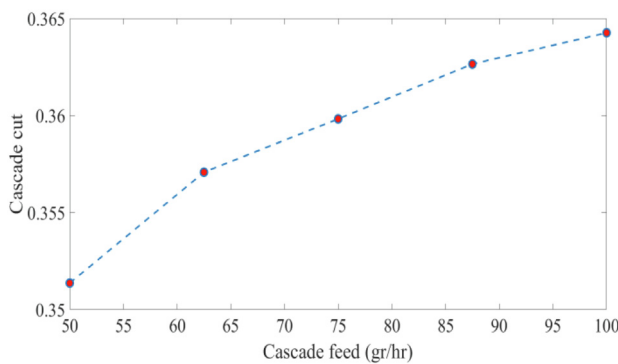
**Fig. 24.** Holdup of the GCs for test case 3.



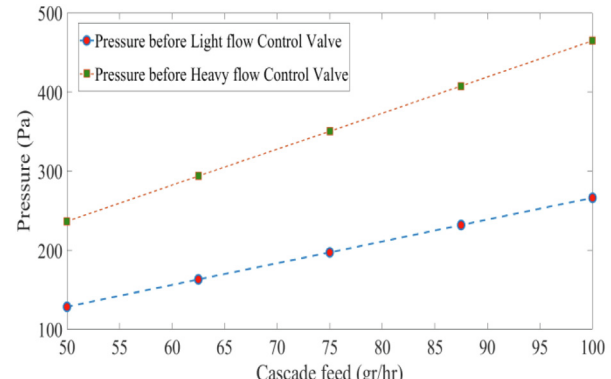
A: Variations of equilibrium time



B: Variations of cascade holdup



D: Variations of cascade cut



A: Variations of output pressure

**Fig. 25.** The variation of equilibrium time, cascade cut, cascade output pressures and total holdup in terms of input feed flow of the cascade.

#### 4.4. Investigation of the effect of feed flow rate on hydrodynamic parameters

**Fig. 25** shows the changes in the cascade equilibrium time, total gas holdup, cascade cut, and the output flow pressure at steady-state by changing the feed flow rate. The input parameters are the same as test case 1. As can be seen, with the increase of the input feed flow to the cascade, all four parameters have increased. With a 50% increase in feed flow from 50 g/h to 100 g/h, the amount of equilibrium time increased by 9%, total holdup increased by 85%, cascade cut increased by 3.5%, light output line pressure increased by 125%, and heavy output line pressure increased by 104%.

## 5. Conclusion

In this paper, the transient simulation of hydrodynamics in taper cascades is presented, and a code named HSSC has been developed. The results of this code analyzed for several different cases. Using this tool, various transient phenomena in cascades can be investigated, such as: commissioning and decommissioning of cascades, different scenarios in adjusting the flow control valves, and sudden changes in the input feed flow. By examining these cases by the code, the following results were obtained.

- 1- If the feed flow enters in a discharged cascade, the gas flow enters through the product and waste scopes of the GCs that are placed adjacent to the feed location stage. Gradually entering of feed flow can reduce these inverse flows.
- 2- During decommissioning, unlike commissioning, the output flows of GCs that are placed adjacent to the feed location stage increases momentarily.
- 3- By using flow control valves on the output pipes of the cascade, which can adjust the desired cascade cut, the values of equilibrium time and total holdup within the cascade are changed.
- 4- As the amount of input feed flow rate to the cascade increases, the cascade cut, the equilibrium time, the pressure of light and heavy lines, and the total holdup increase. For the simulated cascade with 8 centrifuges, with a 50% increase in input feed flow rate from 50 g/h to 100 g/h, the amount of equilibrium time increased by 9%, total holdup increased by 85%, cascade cut increased by 3.5%, light output line pressure increased by 125%, and heavy output line pressure increased by 104%.

## Declaration of Competing Interest

The authors declare that they have no known competing financial interests or personal relationships that could have appeared to influence the work reported in this paper.

## References

- Alam, M., Atta, M.A., Mirza, J.A., Khan, A.Q., 1986. Flow Induced Vibrations in Gas Tube Assembly of Centrifuge. *J. Nucl. Sci. Technol.* 23, 819–827. <https://doi.org/10.1080/18811248.1986.9735059>.
- Amat, S., Hernández-Verón, M.A., Rubio, M.J., 2014. Improving the applicability of the secant method to solve nonlinear systems of equations. *Appl. Math. Comput.* 247, 741–752. <https://doi.org/10.1016/j.amc.2014.09.066>.
- Argyros, I.K., Khattri, S.K., 2013. On the Secant method. *J. Complex.* 29, 454–471. <https://doi.org/10.1016/j.jco.2013.04.001>.
- Azizov, T.E., Smirnov, A.Y., Sulaberidze, G.A., Mustafin, A.R., 2020. Optimization of a system of square cascades for efficient concentration of intermediate isotopes. *J. Phys. Conf. Ser.* 1696, 12010. <https://doi.org/10.1088/1742-6596/1696/1/012010>.
- Emmons, H.W., 2015. Fundamentals of Gas Dynamics. Princeton University Press. <https://doi.org/10.1515/9781400877539>.
- Ezazi, F., Imani, M., Jaber, S., Mallah, M.H., Mirmohammadi, L., 2022. An application of nature-inspired paradigms in the overall optimization of square and squared-off cascades to separate a middle isotope of tellurium. *Ann. Nucl. Energy* 171. <https://doi.org/10.1016/j.anucene.2022.109033>.
- Ezazi, F., Mallah, M.H., Karimi Sabet, J., Norouzi, A., Mahmoudian, A., 2020a. Investigation on the net cascade using Ant Colony optimization algorithm. *Prog. Nucl. Energy* 119. <https://doi.org/10.1016/j.pnucene.2019.103169> 103169.
- Ezazi, F., Mallah, M.H., Sabet, J.K., Norouzi, A., 2020b. A new method for multicomponent mixture separation cascade optimization using artificial bee colony algorithm. *Prog. Nucl. Energy*. 124, 103371.
- Fu, Y., Zeng, S., Hou, Y., 2005. Simulations of the hydraulic status in gas centrifuge cascades. *Qinghua Daxue Xuebao/Journal Tsinghua Univ.* 45, 407–411.
- Hai, W., Xiaojing, L., Weiguo, Z., 2011. Transient flow simulation of municipal gas pipelines and networks using semi implicit finite volume method. *Procedia Eng.* 12, 217–223. <https://doi.org/10.1016/j.proeng.2011.05.034>.
- Imani, M., Aghaie, M., Adelikhah, M., 2021a. Introducing optimum parameters of separation cascades for 123Te using GWO based on ANN. *Ann. Nucl. Energy* 163. <https://doi.org/10.1016/j.anucene.2021.108545> 108545.
- Imani, M., Keshtkar, A., Rashidi, A., Karimi sabet, J., Noroozi, A., 2021b. Simulation of 36S stable isotope enrichment by square single withdrawal cascade. *J. Nucl. Sci. Tech. (JonSat)* 42 (3), 8–17. <https://doi.org/10.24200/NST.2021.1291>.
- Imani, M., Keshtkar, A., Rashidi, A., Karimi sabet, J., Noroozi, A., 2021c. Design and optimization of a tapered cascade for the separation of multi-component mixture by consideration of the hydraulic and operational parameters of the gas centrifuge machine. *J. Nucl. Sci.Tech. (JonSat)*.
- Imani, M., Keshtkar, A.R., Rashidi, A., Sabet, J.K., Noroozi, A., 2020. Investigation on the effect of holdup and cascade shape in NFSW cascades. *Prog. Nucl. Energy* 119. <https://doi.org/10.1016/j.pnucene.2019.103182> 103182.
- Ji, X., Li, P., Sun, J., 2020. Computation of interior elastic transmission eigenvalues using a conforming finite element and the secant method. *Results Appl. Math.* 5. <https://doi.org/10.1016/j.rinam.2019.100083> 100083.
- Khoshechin, S., Mansourzadeh, F., Imani, M., Safridi, J., Mallah, M.H., 2021. Optimization of flexible square cascade for high separation of stable isotopes using enhanced PSO algorithm. *Progress in Nucl. Energy* 140. <https://doi.org/10.1016/j.pnucene.2021.103922>.
- Kiuchi, T., 1994. An implicit method for transient gas flows in pipe networks. *Int. J. Heat Fluid Flow* 15, 378–383. [https://doi.org/10.1016/0142-727X\(94\)90051-5](https://doi.org/10.1016/0142-727X(94)90051-5).
- Malik, M.N., Afzal, M., Tariq, G.F., Ahmed, N., 1998. Mathematical modeling and computer simulation of transient flow in centrifuge cascade pipe network with optimizing techniques. *Comput. Math. with Appl.* 36, 63–76. [https://doi.org/10.1016/S0898-1229\(98\)00141-2](https://doi.org/10.1016/S0898-1229(98)00141-2).
- Manson, Benedict, P.D., Thomas H. Pigford, P.D., Levi, P.D.H.W. 1981. Nuclear Chemical Engineering. Second Edition.
- Mountain, R.D., 2007. Molecular Dynamics Calculation of the Viscosity of Xenon Gas. *Int. J. Thermophys.* 28, 259–267. <https://doi.org/10.1007/s10765-007-0162-6>.
- Mustafin, A.R., Smirnov, A.Y., Sulaberidze, G.A., Borisevich, V.D., Zeng, S., Jiang, D., 2020. Peculiar properties of transient processes in cascades with additional product flow. In: *Journal of Physics: Conference Series*. IOP Publishing Ltd. 1696 (1), 012008.
- Nazeer, M.M., Afzal, M., Tariq, G.F., Ahmed, N., 1999. Global solution algorithm with some assisting techniques for modeling of unsteady flow in centrifuge cascade pipe network. *Comput. Methods Appl. Mech. Eng.* 173, 257–269. [https://doi.org/10.1016/S0045-7825\(98\)00250-3](https://doi.org/10.1016/S0045-7825(98)00250-3).
- Orlov, A.A., Ushakov, A.A., Sovach, V.P., Malyugin, R.V., 2018. Mathematical Modeling of Nonstationary Separation Processes in a Cascade of Gas Centrifuges for Separation of Tungsten Isotopes. *J. Eng. Phys. Thermophys.* 91, 565–573. <https://doi.org/10.1007/s10891-018-1777-0>.
- Palkin, V.A., 2020. Molybdenum Isotope Separation in a Cascade with a Specified Number of Gas Centrifuges in Stages. *At. Energy* 128, 155–161. <https://doi.org/10.1007/s10512-020-00667-7>.
- Shiono, N., Suzuki, H., Saruwatari, Y., 2019. A dynamic programming approach for the pipe network layout problem. *Eur. J. Oper. Res.* 277, 52–61. <https://doi.org/10.1016/j.ejor.2019.02.036>.
- Sulaberidze, G.A., Borisevich, V.D., 2001. CASCADES FOR SEPARATION OF MULTICOMPONENT ISOTOPE MIXTURES. *Sep. Sci. Technol.* 36, 1769–1817. <https://doi.org/10.1081/SS-100104761>.
- Zeng, S., Ying, C., 2001. Transient process in gas centrifuge cascades for separation of multicomponent isotope mixtures. *Sep. Sci. Technol.* 36, 3439–3457. <https://doi.org/10.1081/SS-100107913>.
- Zhao, J., Zeng, S., 2006. Characteristic centrifuge parameters in cascade hydraulics 46, 1577–1580.